Theory and Modeling of Atmospheric Radiative Transfer

6th Semester Project Report

Submitted by

Sahel Mohammad Iqbal

1711112

to the

School of Physical Sciences

National Institute of Science Education and Research

Bhubaneswar

June 7, 2020

ACKNOWLEDGEMENTS

I would first like to thank my project guide, Dr. Jaya Khanna of the School of Earth and Planetary Sciences, for guiding me in this project. Dr. Khanna has been extremely generous with her time and patience, and the interactions that I shared with her are undoubtedly my most valuable experiences from this project. I would also like to sincerely thank Dr. Ashok Mohapatra, Chairperson, School of Physical Sciences, for gracefully agreeing to be my guide from SPS.

Contents

Chapter 1

Introduction

1.1 Why is Radiation Important for our Climate System?

Radiation recieved from the sun is the primary source of energy for almost all processes in the atmosphere. Of the total radiation that the Earth recieves, a small percentage is reflected back out to space, while the rest is absorbed and re-emitted by the Earth. This balance between the incoming radiation from the Sun (which is mostly in the visible range, owing to the Sun's high temperature) and the outgoing radiation from the Earth (mostly in the infrared or longwave region) is what determines the Earth's temperature.

In the absence of an atmosphere, the longwave radiation emitted by the Earth travels to space unimpeded, and the Earth would have an approximate temperature that is much lower than what it is today. With an atmosphere, however, this process gets a whole lot more complicated, because atmospheric particles would now interact with the radiation, primarily through absorption and scattering. Certain gases (which we term greenhouse gases) affect the balance of radiation mentioned above by absorbing and re-emitting the outgoing radiation back to the Earth, thereby increasing the Earth's temperature. This absorption of radiation by atmospheric constituents will heat up the atmosphere as well, and differential heating at different levels of the atmosphere (and the resulting differences in temperatures) is what drives convective processes.

Understanding how radiation propagates through the atmosphere involves understanding the types of particles that are present in the atmosphere, and how each of them interact with radiation. A thorough knowledge of atmospheric radiative transfer is crucial in unravelling the mysteries of several atmospheric phenomena that we see.

The impact of radiative processes on climate can be best explained with an example. It is common knowledge now that temperatures around the world have beeen increasing for the past few decades. Increasing trends have been observed for all three major temperature indices, namely T_{avg}, T_{max} and T_{min} (which are the average, maximum and minimum of temperatures recorded in a day). This is only partially true for India, because here T_{max} is found to be increasing at a much lower rate compared to the other two variables [1]. All

processes that contribute to this anomaly haven't been identified yet, but there is a general consensus among atmospheric scientists that the following prcess is central to the puzzle. Air pollution has reached an uprecedented level in India. Manufacturing industries spew large amounts of aerosols into the atmosphere, and their impact on the Taj Mahal losing its shine by causing acid rains is well documented. An additional role that such aerosols play in the atmosphere is that they reflect a lot of solar radiation, thereby reducing the amount of solar intensity that reaches the Earth's surface. This process is called solar dimming, and is considered to be a major reason of the above mentioned anomaly in India [1, 2].

This project was motivated by the research problem of the role of aerosols and water vapor in heat waves. Both the frequency of occurances and intensities of heat waves in India have been on the rise in the past few years [3], and given the danger that they pose to human and animal well-being, this is a dangerous trend. A proposed hypothesis for this increasing heat wave intensity is an increased heating of the upper atmosphere, due to the presence of aerosols (for which increased pollution is responsible, as described in the previous paragraphs). Aerosols in the atmosphere can act as condensation nuclei for water vapor. Such atmospheric layers containing large amounts of aerosols and water will absorb a high amount of radiation, and will heat up disproportionately compared to its surrounding layers. In the troposphere, which is the region of the atmosphere stretching from the Earth's surface to about 10kms in altitude, temperature decreases with increasing altitude. This temperature gradient allows heat dissipation from the Earth's surface, as hot air would rise up and get replaced by colder air from above. A layer of aerosol and water vapor in the troposphere would interfere with this process, by virtue of its higher temperature. This layer will act as a sort of lid on vertical ventilation - which will not allow hot surface air to rise higher, thus exacerbating heat wave conditions on the surface, and increasing the duration of such episodes. This problem is revisited in Chapter 4.

1.2 Project Outline

The project began with an attempt to understand the basic laws of radiative transfer, with the aim of getting to the heating and emission profiles of the atmosphere. This understanding was then used to create a simple computational model that would take in the density distribution and extinction coefficient values of a particular component of the atmosphere, and would output heating and emission profiles. After this exercise in basic radiative transfer modeling, the next step would be an application of full-fledged radiative transfer models to the problem of heat waves and the radiative role of aerosol and water vapor. A preliminary phenomenological analysis of Indian heat waves was performed which is described in Chapter 4. An analysis of these extreme events using complex radiative

tranfer modeling coupled with atmospheric dynamic modeling was out of the scope of the current project but is recognized as future work.

Chapter 2

Theoretical Basis for Climate - Radiation Interactions

2.1 The Beer-Lambert Law

Given some basic knowledge about a medium - its density and its constituents - we would like to know what fraction of intensity of an incident radiation will make its way across the medium. The physical law which answers this question, the Beer-Lambert law, in its basic form can be written as

$$ln(\frac{I_\lambda}{I_{0\lambda}}) = -\epsilon_\lambda \rho l \tag{2.1}$$

Here I_0 is the incident intensity, I is the transmitted intensity, l is the length of passage of radiation through the medium, ρ is the medium's density (assumed to be a constant) and ϵ_λ is called the extinction coefficient, which is a property of the material(s) comprising the medium. The subscript λ is to emphasize that the extinction coefficient is a wavelength dependent property, and that the above equation holds true only for a given wavelength.

Since I intend to apply this equation for constituents in the Earth's atmosphere, it would be beneficial to write down its differential form, as their densities will be altitude dependent.

$$\frac{dI_\lambda}{dz}(z) = -\epsilon_\lambda \rho(z) I_\lambda(z) \tag{2.2}$$

Intensity here (and throughout this report) refers to monochromatic intensity, which is defined as the light energy crossing a unit area per unit time per unit solid angle per unit wavelength (watts per meter squared per steridian per meter).

The Beer-Lambert law breaks down the dependencies of attenuation into extrinsic (made up of ρ and l) and intrinsic properties (represented by ϵ). The extinction coefficient includes the effects of both absorption and scattering and is a constant for a homogeneous medium and a given wavelength.

Let's picture how the intensity profile for a component in our atmosphere will look. I'll use an incoming solar intensity value I_S of $8.72 * 10^8$ W/m^3sr, which is the Sun's emission intensity at $15\mu m$, and an extinction coefficient value of 0.05 m^2/kg. The density distribution of the component is also needed, which is simply the density profile of the atmosphere multiplied by the mixing ratio profile of the component. For well-mixed gases in the atmosphere (like CO_2), the mixing ratio is constant everywhere. The altitude dependence of Earth's atmospheric density is a decreasing exponential function [4].

$$\rho(z) = \rho_0 \cdot e^{-z/H} \tag{2.3}$$

Here ρ_0 is the density at sea level ($1.225kg/m^3$) and H is the scale height, which is the height over which atmospheric density reduces by a factor of e. The scale height for the atmosphere is close to 8.5km [4], though it may vary with temperature.

With the above mentioned values for the various parameters, and assuming a constant mixing ratio of 1, the intensity distribution has bee plotted in 2.1. Height from the surface of the earth (altitude) is plotted on the y-axis.

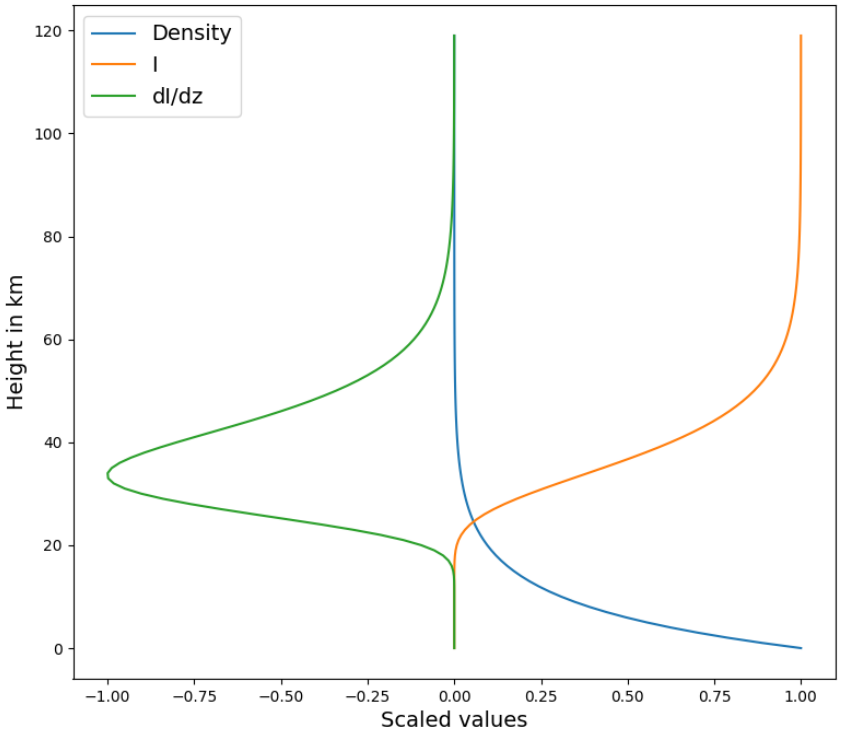

Figure 2.1: Solutions for Beer-Lambert law.

In the above figure, we see that the intensity has dropped to 0 at the surface the

Earth. This is not the case for most of the radiation received from the Sun, however, as the components of the Earth's atmosphere have much smaller extinction coefficients in the shortwave region in which the Sun predominantly emits.

2.2 The Concept of Optical Length

From equation 2.2, it is evident that the rate of absorption the incoming beam is dependent on an effective depth of the medium impacted by both ϵ and ρ, keeping I fixed. This brings us to the concept of optical length, represented by τ, which is defined as

$$\tau(z, S) = \int_S^z \epsilon\rho(z') \cdot dz' \tag{2.4}$$

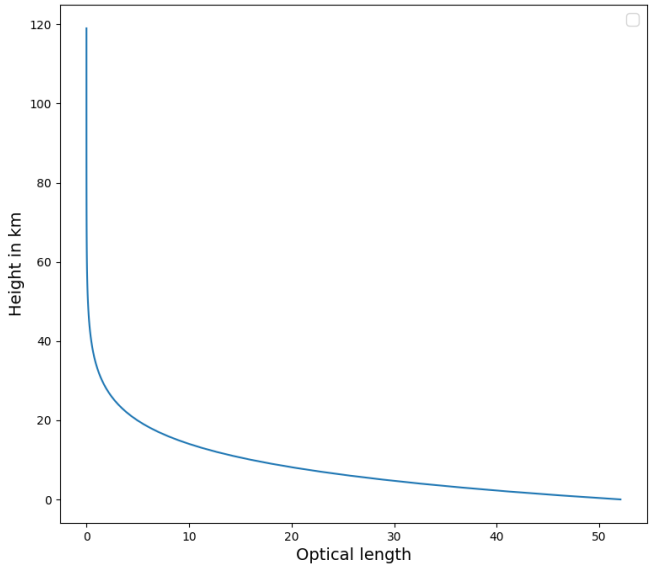

Figure 2.2: Plot of altitude vs optical length for the Earth's atmosphere (density profile of eq. 2.3)

τ is a positive, dimensionless number that can be viewed as a measure of the probability of extinction. Since τ encompasses all of the relevant dependencies for attenuation, it is now the sole property that determines the intensity of transmitted radiation. The solution for Beer-Lambert law can be written in terms of τ as

$$I_\lambda(z) = I_\lambda(S) \cdot e^{-\tau(z,S)} \tag{2.5}$$

Figure 2.3 shows an important property of exponentially decreasing density profiles. The rate of absorption of intensity is maximum at the altitude where the optical depth is 1, which does not necessarily correspond to the altitude with maximum density. While

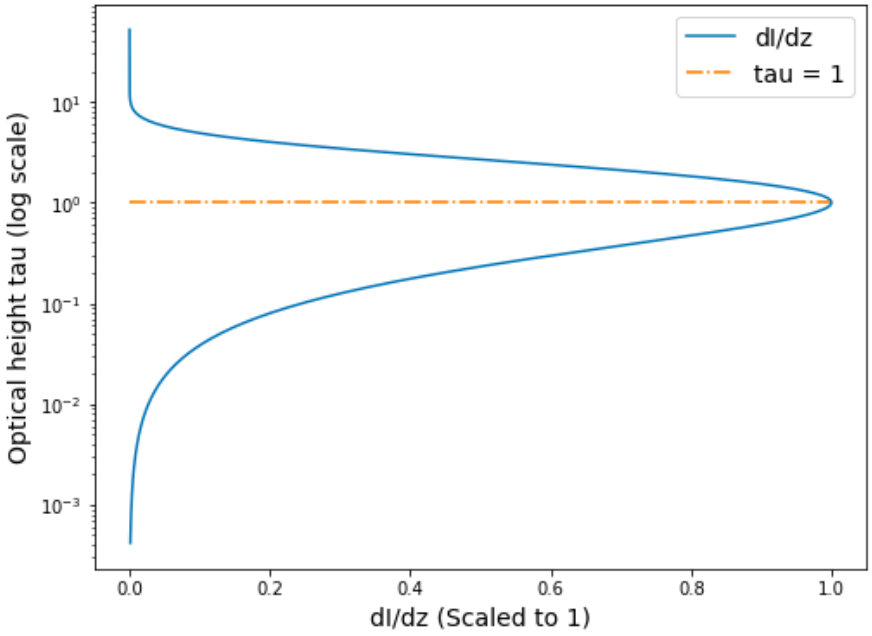

Figure 2.3: Plot of optical height vs dI/dz for exponentially decreasing density profile.

this is not exactly true for the Earth's atmosphere (for reasons which will be discussed in the next section), it still is a good approximation for well-mixed components, and so is a useful concept to keep in mind.

2.3 Schwarzschild's Equation of Radiative Transfer

Figure 2.4 shows how the average surface temperature of the Earth has changed over the past 2000 years. Excluding the period from 1900 onwards, we see that global temperatures have remained more or less stable. This then implies that the Earth must be emitting as much energy as it is absorbing. The atmosphere is mostly transparent to the radiation coming from the Sun, and the Earth absorbs this, heats up and re-emits. But the atmosphere does absorb in the wavelengths emitted by the Earth, and so the atmosphere too heats up and starts to radiate

We'll now add this information to the Beer-Lambert law. The intensity of radiation emitted by a particle/body at temperature T and wavelength λ is given by

$$E_\lambda = e_\lambda \cdot B_\lambda(T) \tag{2.6}$$

where e is the emissivity of the particle and $B_\lambda(T)$ is Planck's intensity function defined as

$$B_\lambda(T) = \frac{2hc^2}{\lambda^5} \frac{1}{\exp(\frac{hc}{\lambda k_B T}) - 1} \tag{2.7}$$

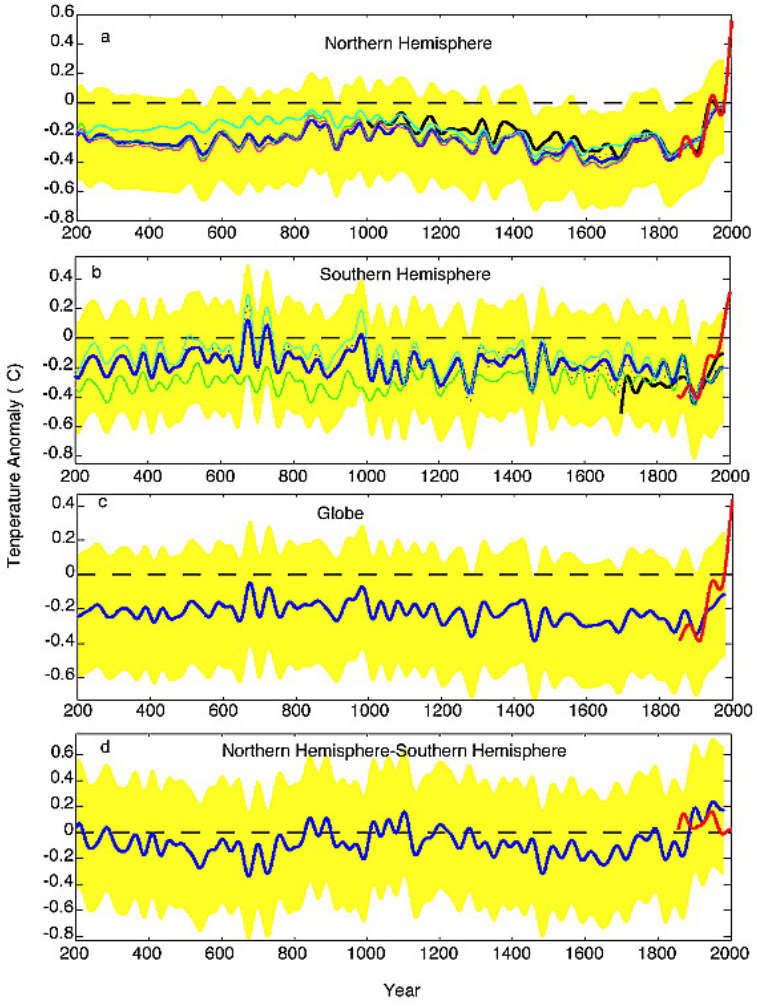

Figure 2.4: Surface temperature anomaly for the past 1800 years [5]. The reference is the average temperature during the period 1961-1990. Anomaly here stands for the difference between the average surface temperature in a given year and the reference value. The shaded yellow region denotes error bars.

h is Planck's constant, c is the speed of light and k_B is Boltzmann's constant. Now let's consider a thin horizontal atmospheric layer that is at an altitude of z above the earth's surface. Assuming this layer to be in thermal equilibrium, Kirchoff's law states that its emissivity and absorptivity must be equal. ie,

$$\alpha_\lambda = e_\lambda \tag{2.8}$$

$$\frac{dI_\lambda}{I_\lambda} = e_\lambda \tag{2.9}$$

Substituting for dI_λ/I_λ from the Beer-Lambert law (eq. 2.2),

$$\epsilon_\lambda \cdot \rho(z) \cdot dz = e_\lambda \tag{2.10}$$

Thus we have found the emissivity of the atmospheric layer. Adding the thermal emission term to Beer-Lambert law yields

$$\frac{dI_\lambda}{dz}(z) = (B_\lambda(T) - I_\lambda(z)) \cdot \epsilon \cdot \rho(z) \tag{2.11}$$

Integrating this equation, we get

$$I(z) = I(S) \cdot e^{-\tau(z,S)} + \int_S^z B(T(z')) \cdot \rho(z) \cdot \epsilon \cdot e^{-\tau(z,z')} dz' \tag{2.12}$$

This is the Schwarzschild's equation of radiative transfer. The first term on the RHS is the transmitted part of the incident intensity, while the second term includes the attenuated thermal radiation coming from every atmospheric layer above the observer.

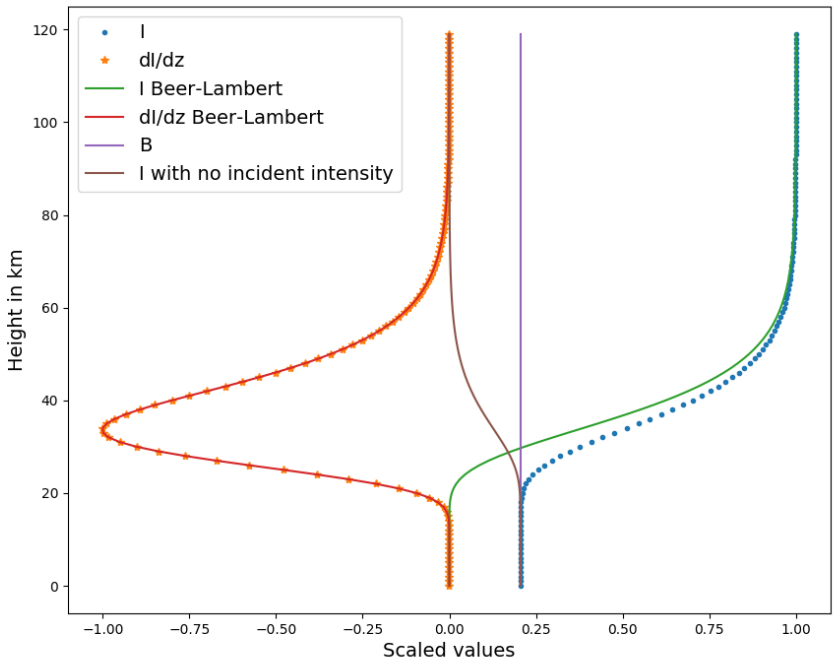

Figure 2.5: Solutions of the Schwarzschild's equation. Solutions of the Beer-Lambert equation are provided for comparison.

In figure 2.5, I've assumed an isothermal atmosphere with a value of B that is around 25% of I_S (intensity from the sun). The key takeaway here is that if the atmosphere is sufficiently dense, then the only radiation that is seen from the surface is that of a perfect blackbody which is at the temperature of the atmosphere. This is all the more surprising because the atmospheric layers themselves do not emit as perfect blackbodies, but instead have an emissivity that is less than 1. Also, because here I assumed the atmosphere to have a constant temperature, the maximum in dI/dz is still at the level of unit optical

depth (not depicted in the figure). This will no longer be the case when dealing with the real atmosphere, which has varying temperatures (and hence varying intensities of emission) at different levels.

2.4 Calculating Vertical Heating Profile

Now that we know how intensity of incident radiation changes throughout the atmosphere, we can now try to address the problem of estimating the vertical heating profile of the atmosphere. We would like to find out the rate of change of temperature of different atmospheric levels, and how it is dependent on the types of atmospheric constituents and their distribution.

The first step here is to find the amount of energy absorbed at each layer. So far in this report, intensity was reported in a unit that is direction dependent (implied by the per steridian). So to find the total energy passing through a unit area oriented in a particular direction, the incident intensity must be integrated over all solid angles, yielding a quantity known as flux density. The flux density, F_λ, is given by

$$F_\lambda = \int_{sphere} I_\lambda(\omega)\cos(\theta)\cdot d\omega \tag{2.13}$$

Here θ is the angle between the incident intensity $I_\lambda(\omega)$ and the area vector of the plane. The flux density has units of watts per square meter per wavelength. The total energy absorbed per unit volume is then the negative of its divergence, $-\nabla\cdot F_\lambda$ (a positive divergence would imply emission). Then we can write

$$\rho\cdot C_p\cdot\frac{dT}{dt} = -\nabla\cdot F_\lambda \tag{2.14}$$

where dT/dt is the rate of change of temperature and C_p is the specific heat capacity of air. Assuming radiation to be unidirectional along the z-axis (in which case the integral from eq. 2.13 can be removed), and a zenith angle of 0 degrees (similar to when the sun is directly overhead), we're left with

$$\nabla\cdot F_\lambda = \frac{dF_\lambda}{dz} = \frac{dI_\lambda}{dz} \tag{2.15}$$

$$\rho\cdot C_p\cdot\frac{dT}{dt} = -\frac{dI_\lambda}{dz} \tag{2.16}$$

Substituting Schwarzschild's equation, we get

$$\frac{dT(z)}{dt} = -\frac{\epsilon}{C_p}(B_\lambda(T(z)) - I_\lambda(z)) \tag{2.17}$$

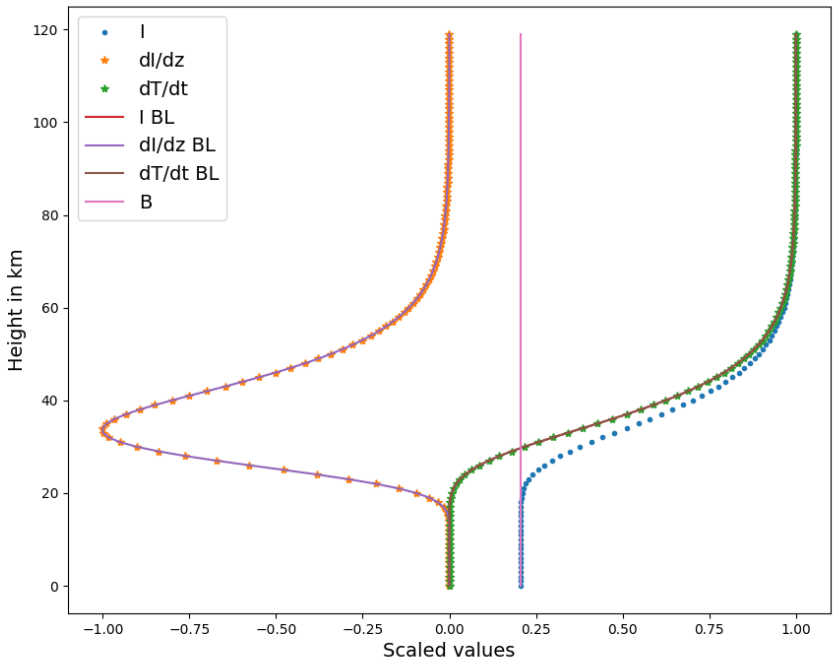

Figure 2.6: Plot with added heating profiles for both Schwarzschild's and Beer-Lambert (BL) equations.

This is the required equation which will tell us the rate of change of temperature at a given altitude. It is dependent on the difference between the incoming radiation I_λ and the outgoing thermal radiation $B_\lambda(T)$, as we would expect.

In figure 2.6, the vertical heating profiles for both the Beer-Lambert and Schwarzschild equations are seen to take the same shape as the intensity solution for the Beer-Lambert law.

2.5 Emission Level and Temperature

Let's now put all of our recently acquired knowledge to use to study something that has great relevance today, climate change. Global temperatures are increasing because the atmosphere is absorbing more and more of the outgoing radiation emitted by the Earth. The objective in this section is to understand how the total radiative energy absorbed by the atmoshpere will change when its composition changes.

Instead of directly looking at the radiation that the atmosphere absorbs, we'll instead work with the total radiation emitted to space by the Earth and the atmosphere as a whole (termed outgoing longwave radiation or OLR). As the incident radiative energy from the Sun is more or less constant (subject to seasonal variations), an increase (decrease) in

OLR will imply a decrease (increase) in the amount of radiation absorbed, and so OLR is a good proxy to use.

The intensity of emission by any single atmospheric layer has been calculated already, and is given by

$$E_\lambda(z) = \epsilon_\lambda \cdot \rho(z) \cdot dz \cdot B_\lambda(T(z)) \tag{2.18}$$

As they travel upwards towards the top of the atmosphere (TOA), these em waves undergo attenuation according to Beer-Lambert law, and the intensity recieved at TOA from a layer in the atmosphere can be written down as

$$Q_\lambda(z) = E_\lambda(z) \cdot e^{-\tau(z,S)} \tag{2.19}$$

The altitude corresponding to the layer with maximum $Q_\lambda(z)$ is called the emission level (EL). This is an important quantity because the OLR that is received at TOA will be characteristic of the temperature of the EL. Studying the changes in EL (and thereby emission temperatures) brought on by an increase in concentration of greenhouse gases may provide valuable insight and evidence of global warming, and this concept is put to use in the next chapter.

Chapter 3

Results from the Computational Model

3.1 The Need for Numerical Modeling of Atmospheric Radiative Processes

The equations that govern certain radiative processes were described in the previous chapter. A reliable way to solve them for real atmospheric conditions, regardless of their analytical complexity, is to use a numerical method using computers. An atmospheric radiative transfer model is simply a piece of code which takes in certain boundary conditions and parameters of the atmosphere, solves the differential equations of radiative transfer by employing numerical integration, and returns variables of interest like the total outgoing intensity from the Earth and the rate of heating of atmospheric layers. In fact, these algorithms are often used in the reverse order - to back-calculate atmospheric temperatures and molecular species distributions from the total outgoing radiation and other parameters which can be directly measured by satellites.

3.2 General Information Regarding the Model

The model was implemented in Python, and I used a finite difference numerical integration technique called Euler's method to solve the relevant differential equations.

The results obtained in this chapter are only considering the effects of carbon dioxide in the atmosphere. I chose to study CO_2 because of the following reasons:

- It is one of the most important greenhouse gases apart from water.
- It has a narrow and distinctive range of wavelengths in which it absorbs.

The model considers emission by both the Sun and the Earth.

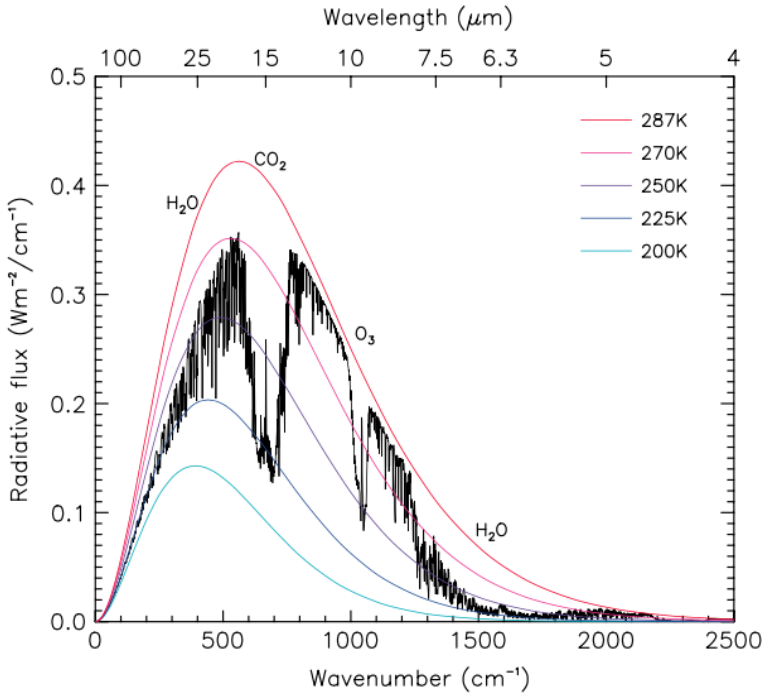

Figure 3.1: Outgoing radiation spectrum of the Earth [6]. The effect of different compounds on the Earth's emission spectrum can be seen. The CO_2 absorption band centered around $15\mu m$ is strikingly evident.

3.2.1 Extinction Coefficient Values

The data required to calculate extinction coefficient values for CO_2 at different wavelengths were obtained from an online database called HITRAN [7]. The relevant data was accessed and extinction coefficients were found using functions made available in the HAPI python library [8].

3.2.2 Density Profile

CO_2 is a relatively well-mixed gas, which means that its concentration as a percentage of total air molecules (by both weight and volume) remains constant throughout the atmosphere. As a result, the density distribution for CO_2 can be obtained by multiplying the atmosphere's density distribution with CO_2's mixing ratio.

3.2.3 Temperature Profile

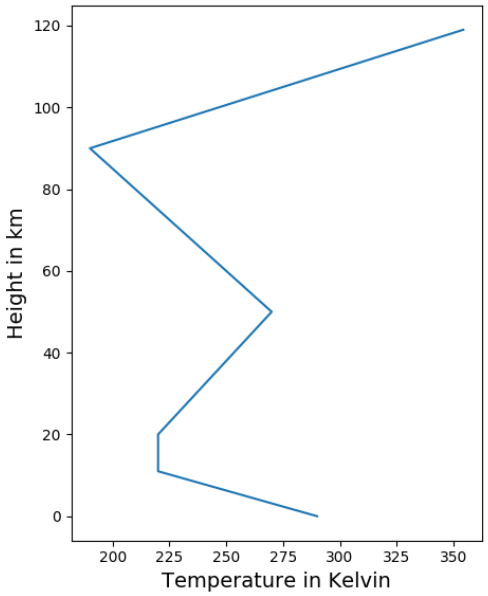

Figure 3.2: Approximate temperature profile of the earth.

The temperature profile that was used to generate the following models is given in figure 3.2. This is a slightly idealized model of the real temperature profile of the atmosphere, as in reality the temperature gradients are not linear everywhere.

3.3 Heating Profile of the Atmosphere

As I briefly mentioned in the Introduction chapter, the differences in the rate of heating of different atmospheric layers is the energy source of almost all major convective processes in the atmosphere. Hence it is important for us to understand how the presence of an absorber and a change in its concentration can alter atmospheric thermodynamics and consequently atmospheric dynamics. In this example we will see that an idealized concentration of CO_2 in an idealized atmosphere produces strong radiative heating. An increase in atmospheric aerosols or water-vapor can have the same impact as they are also strong absorbers of outgoing longwave radiation.

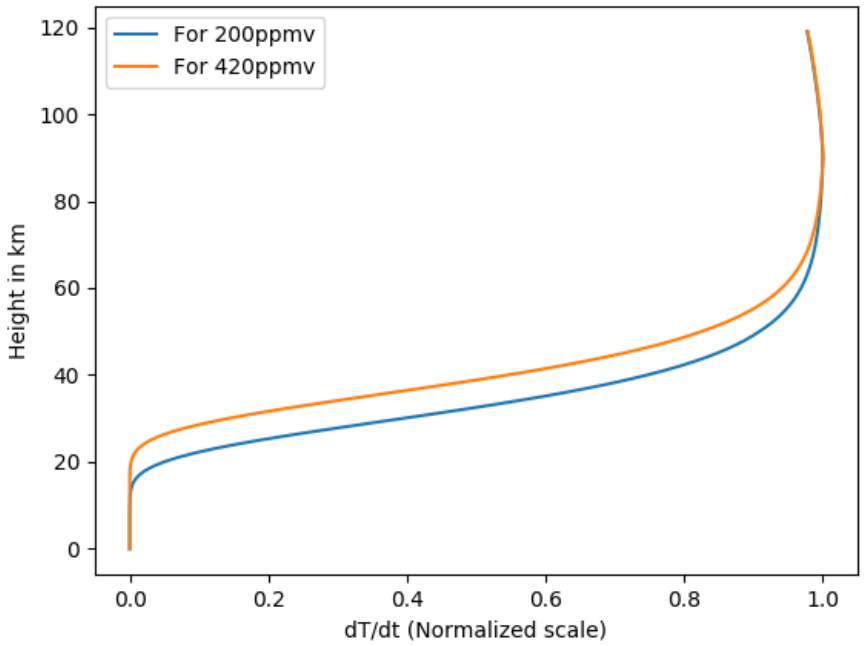

Figure 3.3: Heating profile of the atmosphere at $15\mu m$ for CO_2.

The heating profile of the atmosphere at one particular wavelength for two different concentrations of CO_2 is given in figure 3.3. We see that because CO_2 strongly absorbs in this wavelength, it does contribute to atmospheric heating. The difference between the two plots is representative of the fact that changing the concentrations of absorbers can have a significant impact on the heating profile of the atmosphere.

3.4 Emission Temperature of the Earth

Suppose we would like to find out the impact of increasing carbon dioxide concentration in the atmosphere. There are many facets to this, and one of them is the effect on outgoing longwave radiation.

Let's first consider a single wavelength. The OLR intensity at $15\mu m$ for CO_2 is plotted in figure 3.4. It has been plotted for two different atmospheric concentrations of CO_2 - 420 parts per million by volume (ppmv), which is the current level, and 200 ppmv.

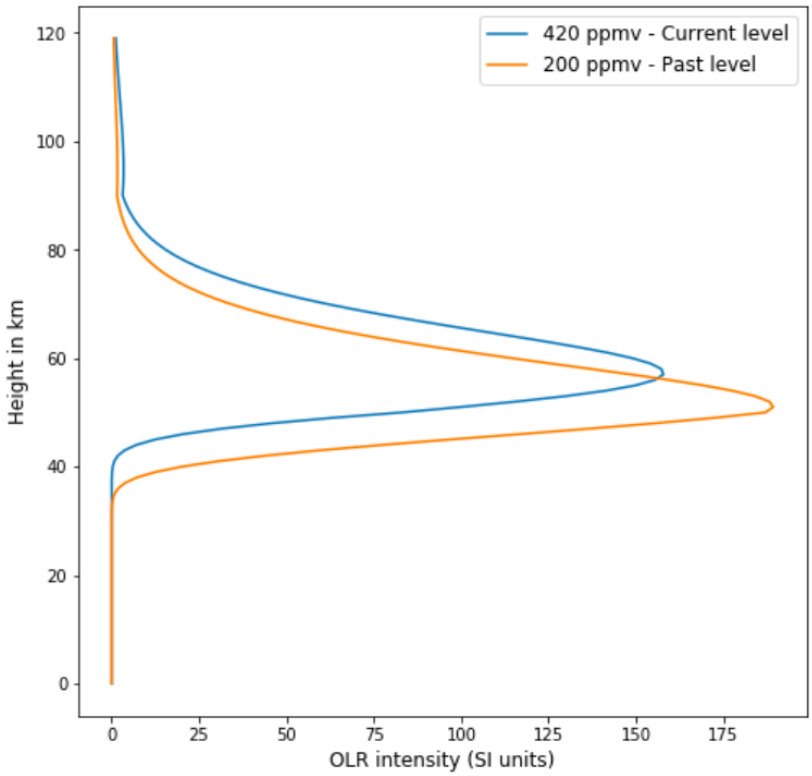

Figure 3.4: Plot of OLR intensity at $15\mu m$ for CO2.

The peaks of the two plots represent their corresponding emission levels. The emission level for 200 ppmv is at 51km altitude with a temperature of 268K, while that for 420 ppmv is at 57km with a temperature of 256K. Thus we see that as CO_2 concentration has gone up, the temperature of the emission level has gone down.

A lower emission level temperature causes a lower intensity of OLR, which means that the atmosphere retains a larger portion of the energy emitted by the earth at this particular wavelength. This would cause the average temperature of the Earth's atmosphere to rise.

Let's now look at the emission level temperatures at a range of wavelengths, for three different CO_2 concentrations. This is given in figure 3.5.

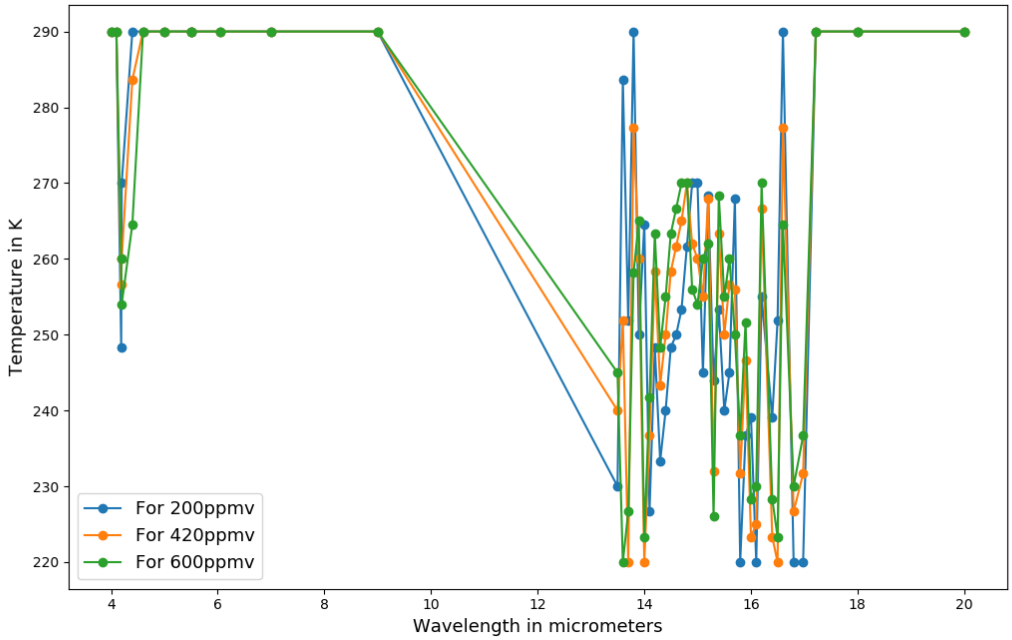

Figure 3.5: Plot showing variation of emission temperature with wavelength for different atmospheric concentrations of CO2.

In the above figure, we see that outside a wavelength range of about 14-17μm (and a very narrow region in the left end), the emission temperature is 290K irrespective of CO_2 concentration. What does this mean? 290K is the surface temperature of the Earth. This means that the radiation coming from the Earth's surface is travelling relatively unimpeded through the atmosphere, because in these wavelengths CO_2 does not absorb or emit much. Things get interesting, though, when we look at the wavelength region in which CO_2 does absorb. This region is plotted in figure 3.6.

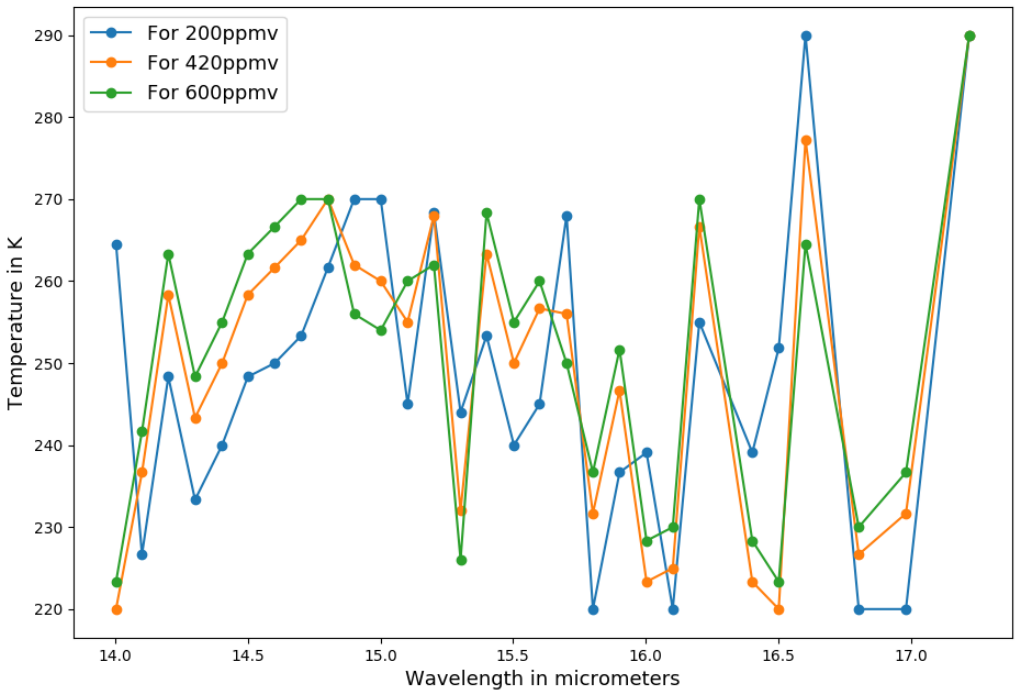

Figure 3.6: Zooming in on the $14 - 17\mu m$ wavelength range of figure 3.5.

When looking at figure 3.6, keep in mind that a higher emission temperature is favorable (going with the logic that we don't want the atmosphere's temperature to rise further). For $15\mu m$, we observe that ET(600ppmv) $<$ ET(420ppmv) $<$ ET(200ppmv) (ET stands for emission temperature). We saw the same result in figure 3.4. However, look either a bit to the left or a bit to the right of $15\mu m$, and there the trend has reversed. ie, ET(200ppmv) $<$ ET(420ppmv) $<$ ET(600ppmv). This inversion is taking place several times in the graph.

This imparts a very valuable lesson. An increase in CO_2 concentration does not affect every wavelength equally. The atmosphere will absorb more energy at some wavelengths, and less at others, for every different concentration of CO_2. So to understand the net change in global temperatures, we'll need to consider the effects at every wavelength.

Chapter 4

Impacts of Radiative Interactions on Atmospheric Dynamics and Climate

By this point, I've already mentioned multiple times that the energy provided by the Sun's radiation, and the in-homogenous absorption of this incident energy by different layers of the atmosphere, form the foundation of all climate processes. In that sense radiative transfer could be termed as the most important driver and regulator of climate because its thermal impacts are enormous.

A vertically inhomogeneous anomalous heating due to a change in any radiatively active atmospheric component can be consequential for vertical mixing and hence near surface climatic conditions, as we saw in the Introduction chapter. This is a key understanding behind the evolution of the hypotheses that motivated this project on the role of aerosols and water vapor on near surface heat wave conditions – that a spatially heterogenous increase in aerosol emission, their near surface trapping and their subsequent role as cloud condensation nuclei in a warm and humid atmosphere under climate change might have an effect on near surface heat wave conditions. This hypothesis is supported by the fact that both aerosols like black carbon, and water vapor are strong absorbers of the outgoing longwave emission from the Earth.

This hypothesis is supported by observations like that shown in Figure 4.1. Usually heat waves are caused due to abnormal high pressure areas that fixate over large swaths of land. The surface responds by heating up due to non-convective, clear sky, stable conditions associated with the high pressure. A comparison of figure 4.1 with a topography map of the country shows that the spatial distribution of the heat wave hot spots corresponds to low laying topographical regions. This suggests the trapping of some conditions within the valley boundary layer that exacerbate the heat wave. Aerosol pollution and subsequent cloud seeding could be one such component.

Many indepth experiments with observational and numerically simulated data would

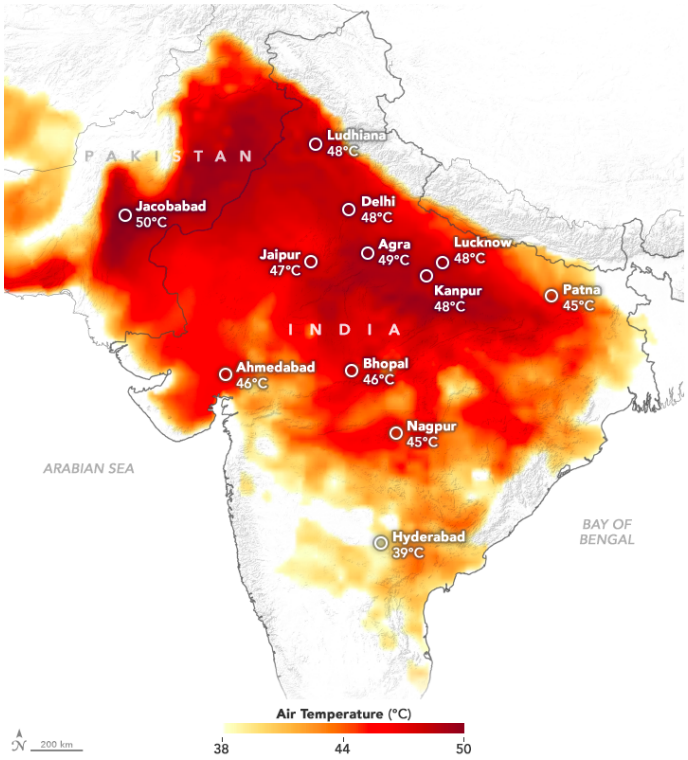

Figure 4.1: Severely affected regions of the 2019 heat wave in India [9].

be required to test the above hypothesis. In this project I worked with only a couple observational proxy data for aerosol concentration and water vapor. In the process I became acquainted with different types of datasets used in climate sciences – such as ground based measurements from IMD, satellite based AIRS dataset and reanalysis data from MERRA [10]. I also acquaninted myself with the acquisition, reading, plotting and interpretation of these climate datasets. The timeline of the project limited the analysis that could be performed with this data to test the above hypothesis, however, the results obtained (however basic) were encouraging and are summarized below.

Figure 4.2 shows aerosol optical depth data during a heat wave in India in 2015. As is clear from the figure, aerosols are concentrated over the low-lying Indo-Gangetic plains. This behavior is expected as aerosols have higher density compared to other atmospheric constituents, and will seek out low terrains by the action of gravity alone. Comparing this with figure 4.1, we see that cities lying in the same region, which include Patna, Lucknow, Kanpur, Delhi, Agra, Ludhiana and Jacobabad, have reported the highest temperatures during the heat wave.

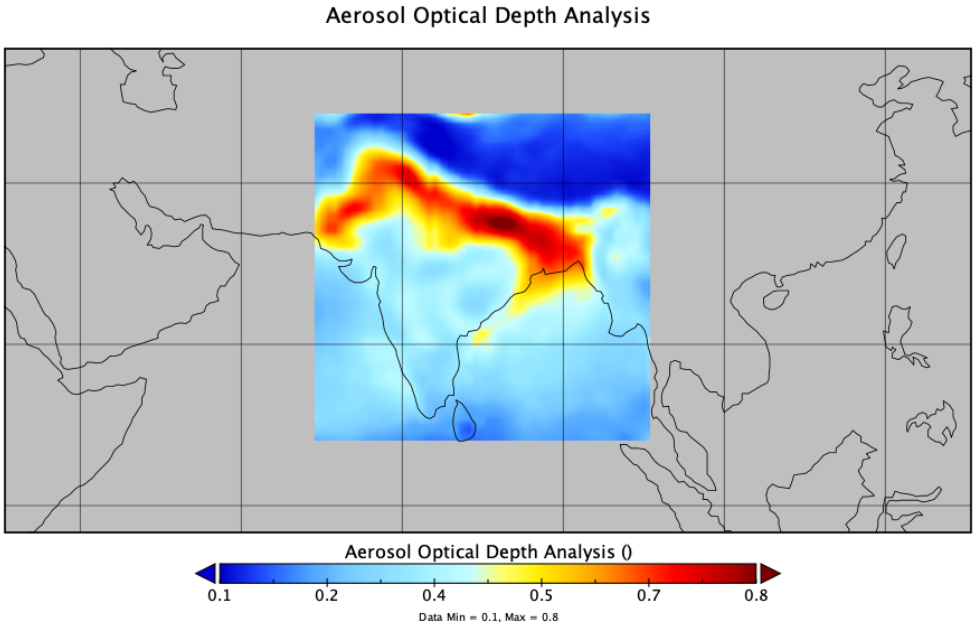

Figure 4.2: The monthly mean of aerosol optical depth values over India in May 2015. Aerosol optical depth is a quantitative measure of the amount and distribution of aerosols in the atmosphere, and this figure is indicative of high pollution levels in the northern plains. The 2015 heat wave took the lives of over 1500 people. Data from MERRA [10], plotted using Panoply [11].

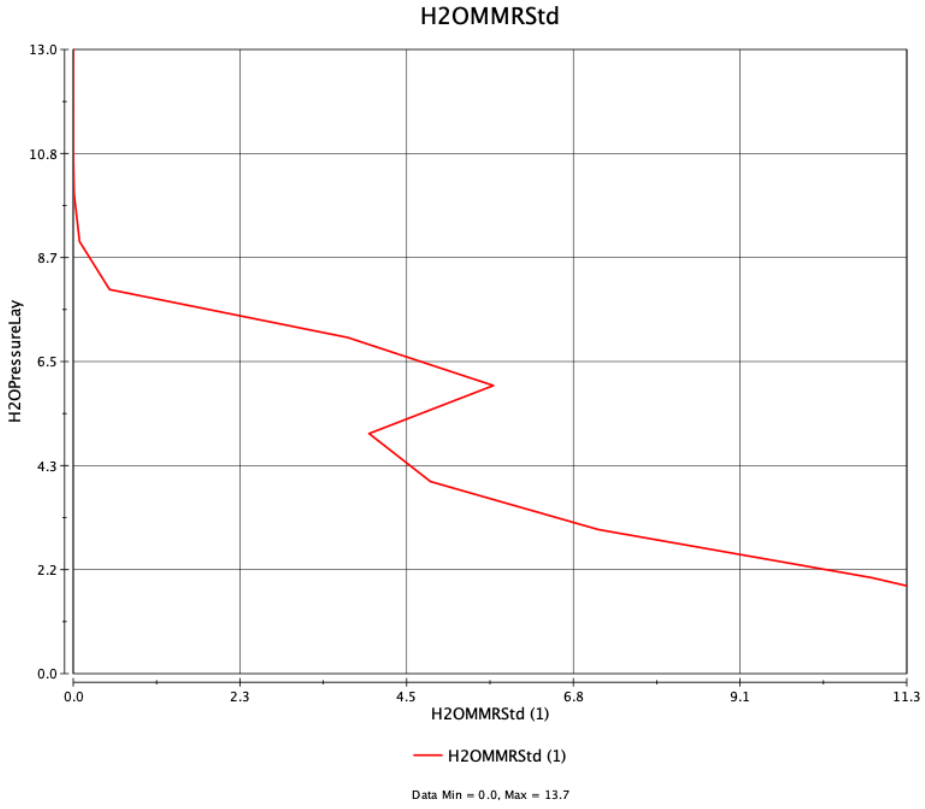

Figure 4.3: Water vapor concentration over Hyderabad in May 2015. Data from MERRA [10], plotted using Panoply [11].

Figure 4.3 shows the vertical profile of water vapor over Hyderabad for a day during the same heat wave. The y-axis of the plot, 'H20PressureLay', is representative of altitude, and 'H20MMRStd' on the x-axis is a measure of concentration. Note the spike in water concentration close to the middle of the plot. This atmospheric layer with a high water content will will be at a higher temperature than the levels immediately below it, because it will absorb more radiation coming from the Earth. This is an ideal representation of the lid effect which I explained in the introduction, wherein hot surface air gets stuck underneath.

These last two figures show a higher incidence of aerosols and water vapor above areas which were severely affected by heat waves. This suggests a possible correlation between the two, and it is worth exploring this possibility further.

Chapter 5

Limitations and Future Work

This simple model that was built with only the most fundamental laws can now give us heating and emission profiles and the outgoing spectra of the Earth. However, it is important to understand the limitations and shortcomings of this model, so that its results can be read within the proper context.

Let's first check the accuracy of this model, by comparing some predicted parameters with known values. In the previous chapter, I obtained an emission level of 57kms for 420ppmv of CO_2, while the actual value is closer to 25kms [6]. This model only takes into account absorption and isotropic scattering by atmospheric particles, which are both accounted for by the extinction coefficient. However, other processes such as non-isotropic scattering. As an example of how these processes may affect the atmospheric radiation profile, consider the process of reflection. Different percentages of the incoming solar radiation are reflected back into space by atmospheric particles (exactly how much is reflected is dependent on wavelength), and the reflected radiation plays no further role in the atmosphere. This is not accounted for in this model.

Another major functionality that can be added is to include dynamical processes such as convection, which plays the primary role in redistributing heat and particles is redistributed throughout the atmosphere. This improvement would go a long way in helping the model make testable real world predictions, which remains the ultimate goal.

Here I present a method to test the hypothesis presented in chapter 4. Satellite measurements of vertical profiles of aerosols and water can be compared at locations experiencing heat waves to check if these spikes in concentration at the same altitudes. If yes, then this indicates that there might be a connection between the two, and we can move on the next step. This would involve inputing the vertical profile data to a fully fledged atmospheric model (which combines both radiative and dynamical aspects) and validating the output against in situ measurements.

Bibliography

1. Kumari, B., Londhe, A., Daniel, S. & Jadhav, D. Observational evidence of solar dimming: Offsetting surface warming over India. *Geophysical Research Letters - GEOPHYS RES LETT* **34.** doi:10.1029/2007GL031133 (Nov. 2007).
2. Wild, M., Ohmura, A. & Makowski, K. Impact of global dimming and brightening on global warming. *grl* **34.** doi:10.1029/2006GL028031 (Feb. 2007).
3. P, R., Rajeevan, M. & Srivastava, A. On the Variability and Increasing Trends of Heat Waves over India. *Scientific Reports* **6,** 26153 (May 2016).
4. Fu, Q. in *Atmospheric Science (Second Edition)* (eds Wallace, J. M. & Hobbs, P. V.) Second Edition, 113–152 (Academic Press, San Diego, 2006). ISBN: 978-0-12-732951-2. doi:https://doi.org/10.1016/B978-0-12-732951-2.50009-0. http://www.sciencedirect.com/science/article/pii/B9780127329512500090.
5. Mann, M. & Jones, P. Global Surface Temperatures over the Past Two Millennia. *Geophysical Research Letters* **30.** doi:10.1029/2003GL017814 (Aug. 2003).
6. Zhong, W. & Haigh, J. The greenhouse effect and carbon dioxide. *Weather* **68,** 100–105 (Apr. 2013).
7. Gordon, I. *et al.* The HITRAN2016 molecular spectroscopic database. *Journal of Quantitative Spectroscopy and Radiative Transfer* **203.** HITRAN2016 Special Issue, 3–69. ISSN: 0022-4073 (2017).
8. Kochanov, R. *et al.* HITRAN Application Programming Interface (HAPI): A comprehensive approach to working with spectroscopic data. *Journal of Quantitative Spectroscopy and Radiative Transfer* **177.** XVIIIth Symposium on High Resolution Molecular Spectroscopy (HighRus-2015), Tomsk, Russia, 15–30. ISSN: 0022-4073 (2016).
9. Patel, K. *Heatwave in India* https://earthobservatory.nasa.gov/images/145167/heatwave-in-india.
10. *Global Modeling and Assimilation Office (GMAO) (2008), MERRA 2D IAU Diagnostic, Single Level Meteorology, Monthly Mean V5.2.0, Greenbelt, MD, USA* doi:10.5067/W3UEUC5V7M9M. https://disc.gsfc.nasa.gov/datasets/MATMNXSLV%5C_5.2.0/summary?keywords=merra.
11. Schmunk, R. *NASA GISS: Panoply 4 netCDF, HDF and GRIB Data Viewer* https://www.giss.nasa.gov/tools/panoply/.